applied sciences

MDPI

Article

Multi-Objective Optimization of Voltage-Stability Based on Congestion Management for Integrating Wind Power into the Electricity Market

Jin-Woo Choi and Mun-Kyeom Kim *

Department of Energy System Engineering, Chung-Ang University, 84 Heukseok-ro, Dongjak-gu, Seoul 156-756, Korea; spjw11@naver.com

* Correspondence: mkim@cau.ac.kr; Tel./Fax: +82-2-5271-5867

Academic Editors: Amjad Anvari-Moghaddam and Josep M. Guerrero
Received: 7 April 2017; Accepted: 30 May 2017; Published: 2 June 2017

Abstract: This paper proposes voltage-stability based on congestion management (CM) for electricity market environments and considers the incorporation of wind farms into systems as well. A probabilistic voltage-stability constrained optimal power flow (P-VSCOPF) is formulated to maximize both social welfare and voltage stability. To reflect the probabilistic influence of CM in the presence of wind farms on voltage stability, Monte Carlo simulations (MCS) are used to analyze both the system load and the wind speed from their probability distribution functions. A multi-objective particle-swarm optimization (MOPSO) algorithm is implemented to solve the P-VSCOPF problem. A contingency analysis based on the voltage stability index (VSI) for line outages is employed to find the vulnerable line of congestion in power systems. The congestion distribution factor (CDF) is also used to find the optimal location of a wind farm in CM. The optimal pricing expression, which is obtained, with respect to preserving voltage stability, by calculating both the locational marginal prices (LMPs) and the nodal congestion prices (NCPs), is demonstrated in terms of congestion solutions. Simultaneously, the voltage stability margin (VSM) is considered within the CM framework. The proposed approach is implemented on a modified IEEE 24-bus system, and the results obtained are compared with the results of other optimal power flow methods.

Keywords: congestion management; probabilistic voltage-stability-constrained optimal power flow; congestion distribution factor; voltage stability margin; multi-objective particle swarm optimization; wind farm

1. Introduction

Congestion management (CM) is one of the most critical transmission problems of open access environments [1]. Congestion occurs in a power market if the transmission system is incapable of adjusting all of the desired transactions because of the existence of system violations [2]. System congestion may also threaten the reliability of the power system by making it more vulnerable to sudden disturbances. It may also impede market efficiency, forcing consumers to reduce their electric power consumptions because of the rises in market prices. As the organizations responsible for maintaining power system security efficiently, independent system operators (ISOs) have to mitigate congestion problems by using market-based tools and/or effective operating facilities [3]. Market-based techniques using both locational marginal prices (LMPs) and nodal congestion prices (NCPs) have been proposed to manage and relieve transmission congestion [4]. The LMP is the generation marginal cost of meeting both the power demands and the transmission losses at a specific node, and the NCP is the cost of satisfying network security parameter limits. Consequently, the market price structure both provides the marginal cost of generating units and indicates the system

security cost of the power network. Thus, it is currently used by ISOs as well as many researchers as CM pricing [5,6]. In addition, the influence of CM can be analyzed through the results obtained from LMPs and NCPs.

Recently, wind energy has emerged as a critical candidate for bridging the gap between global power supply and demand [7]. Wind energy is primarily considered as a sustainable method of mitigating severe problems that result from the use of fossil fuels, such as market volatility, social conflict, and global warming [8,9]. Hence, special attention should be paid to wind energy sources in the CM of the electricity market. CM is essential to the efficient operation of any electricity market, with a special emphasis on wind energy. Assume that several buses in a power system each have strong potential for wind installation. An ISO should consider several factors in determining the optimal placements for wind farms in order to alleviate transmission congestion via additional power injection. CM that uses proper power injection reduces both the component of the LMP associated with the congestion price and reduces transmission losses. Several CM problems involving renewable energy sources have been analyzed in the literature [10–12]. In [10], the authors proposed a new optimal model of congestion management with an emphasis on the promotion of renewable energy sources in a competitive electricity market. In [11], the CM problem incorporated a wind farm based on the sensitivity factor. In [12], the authors addressed transmission congestion relief by considering both the sizes and the sites of new renewable energy sources. However, the impact of renewable energy congestion relief on the probabilistic approach was not considered. Wind behavior is often unpredictable, as it is a stochastic phenomenon. In particular, wind speed is highly dependent upon the weather conditions, geographical region, and season. Wind farms, which deploy many wind turbine generators to harness wind energy for electricity production, have a variable power outputs due to variations in wind speed [13]. Therefore, the rapid global growth of wind power capacity may increase the uncertainties for congestion problems. A reliable probabilistic method that can consider random wind speeds must be found to solve congestion problems.

CM is essentially an optimization problem with an exponential number of constraints that can be generally described as an optimal power flow (OPF) problem whose objective function is the maximization of social welfare and whose constraints are the load flow equations and the operation limitations [14]. In [15], the authors applied CM to the adjustments of power transfers in transmission lines based on a transmission congestion penalty-factor. A CM method based on OPF, presented in [16], relieved congested transmission lines by using both power generation rescheduling and load curtailment. In [17], the authors analyzed both the enhancement of voltage loadability and the transmission mechanisms of line outage contingencies in a smart power network and found that if a few lines were able to be fully loaded, some voltages could be adjusted to their lower restrictions. Although no violation occurred, even a small disturbance, such as a load change, could cause the system to deteriorate into an unstable condition.

As the penetration of wind energy into a power network increases, the influence of wind turbines on the voltage stability becomes more significant. Following a large incorporation of wind power into a grid, severe problems may arise due to both the characteristics of the wind generators and the random nature of wind. Hence, when wind power systems are connected to weak networks, the voltage stability should be considered in addition to the uncertainties of the wind power in their CM frameworks. Voltage stability refers to the ability of a power system to sustain steady levels of voltage for all of the network buses after being subjected to a disturbance [18]. Voltage instability can lead to load shedding, branch trips, or even cascading outages caused by acting protective relays. Voltage collapse is a phenomenon in which a sequence of voltage instability events leads to a blackout. Generally, the closeness to voltage collapse can be used to measure the voltage stability of a power system. In systems with weak connections among areas, congestion problems frequently occur due to either overloading or voltage security requirements. Several techniques have been proposed to solve voltage security problems in CM. In [19], a multi-objective method was presented to maximize both the social benefits of the power market and the distance to the maximum loading point. In this

method, which employed a loading margin, the ISO paid more for security enhancement. In [20], a method for ensuring voltage security after the implementation of CM was proposed. However, it did not consider the diverse effects of different loads on the voltage security. In addition, due to the complexities of power-system stability problems, both the solution spaces resulting from inter-area power transfer problems and the system stability boundaries may become complicated. As such, traditional optimization techniques can occasionally fail or encounter numerical difficulties with objective functions. In contrast, both particle swarm optimization (PSO) and differential evolution are powerful population-based searching algorithms [21]. However, transforming a typical single-objective PSO into a multi-objective PSO requires reestablishing both the best local and global individuals to seek a front of optimal solutions.

In this paper, we propose an approach to solving CM problems, focusing in particular on both voltage stability and wind farms in the electricity market. The problem is modeled as a probabilistic voltage-stability constrained optimal power flow (P-VSCOPF) to maximize both the social welfare and the voltage stability margin. A multi-objective particle swarm optimization (MOPSO) algorithm is used to determine the P-VSCOPF solution for mitigating the transmission congestion problem. Since wind speed is a random variable and load forecasting contains uncertainties as well, we apply a probabilistic approach based on Monte Carlo simulations (MCSs). The contingency analysis for line outages is also considered by using the voltage stability index (VSI). The optimal sites of wind farms are determined based on the congestion distribution factor (CDF), and the voltage stability margin (VSM) is considered within the CM framework. Simultaneously, optimal pricing expressions for relieving congestion are derived with linear programming (LP).

2. Uncertainty Analysis and Wind Farm Modeling

2.1. Wind Speed

Wind speed is a random variable, and its fluctuations over a period are expressed by probability distribution functions. In general, wind speed can be described using either a two-parameter Rayleigh or a Weibull distribution [22]. The Rayleigh distribution is the simplest distribution used to describe average wind speed because it has only a single model parameter: b. Its probability distribution and cumulative distribution functions are, respectively,

$$f_{S_w}(S_w;b) = \frac{S_w}{b^2}\exp\left(-\frac{1}{2}\frac{{S_w}^2}{b^2}\right) \tag{1}$$

and

$$F_{S_w}(S_w;b) = 1 - exp\left(-\frac{1}{2}\frac{{S_w}^2}{b^2}\right) \tag{2}$$

As a distribution recommended in literature, the Weibull distribution is also widely utilized to both represent wind speed distribution and compute wind energy potential [23]. It is thought to fit the probability distribution for wind speed better than the Rayleigh distribution does because of its more flexible shape granted by its additional parameter. The probability density function of the Weibull distribution is formulated as

$$f_{Sw}(S_w;k,a) = \frac{kS_w^{k-1}}{a^k}\exp\left[-\left(\frac{S_w}{a}\right)^k\right],\ S_w > 0, \quad k,a > 0. \tag{3}$$

The Weibull distribution has a two-parameter function characterized by both a and k. These parameters determine the wind speed necessary for the optimum performance of a wind-energy conversion system. A survey of the literature indicates that the shape parameter of the Weibull distribution for estimating the global wind energy conditions ranges from 1.2 to 2.75. The cumulative

distribution function of the Weibull distribution, which gives the probability of the wind speed, is expressed as

$$F_{S_w}(S_w; k, a) = 1 - exp\left[-\left(\frac{S_w}{a}\right)^k\right] \tag{4}$$

2.2. System Load

To reflect a proper probabilistic approach, the uncertainty in the system load must be considered. The pattern of the system load is assessed by accumulating the consumption periodically over daily, weekly, or monthly periods. Uncertainties related to the predicted load data are usually considered by using a normal distribution with a standard deviation. A normal probability distribution function can be expressed as

$$f_L(P_L) = \frac{1}{\sqrt{2\pi{\sigma_L}^2}} exp\left[-\frac{(P_L - e_L)^2}{2{\sigma_L}^2}\right] \tag{5}$$

2.3. Wind Turbine Modeling

The power output of a wind turbine is associated with the wind speed, which is converted to electrical power by different types of wind turbine generators. Our model representing a wind turbine's power is given by

$$P_w(S_w) = \begin{cases} 0 & S_w < S_{cut-in} \\ P_{w,rated}\frac{S_w^2 - S_{cut-in}^2}{S_{rated}^2 - S_{cut-in}^2} & S_{cut-in} < S_w < S_{rated} \\ P_{w,rated} & S_{rated} < S_w < S_{cut-out} \\ 0 & S_w > S_{cut-out} \end{cases} \tag{6}$$

Figure 1 shows the representative power curve for a wind turbine. The cut-in wind speed S_{cut-in} is the minimum speed required to generate power. If the wind speed reaches the cut-in value, power is generated by the wind turbine. The generator produces the machine's rated power $P_{w,rated}$ when the wind speed reaches the rated wind speed S_{rated}. As shown in Figure 1, power production is almost constant between S_{rated} and $S_{cut-out}$. At the cut-out wind speed $S_{cut-out}$, power generation is shut down to protect the wind turbine from damage and defects, and the power output becomes zero.

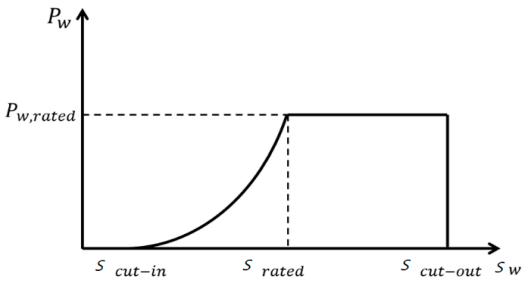

Figure 1. Wind turbine power curve.

Recently, both permanent magnet synchronous generators (PMSGs) and doubly fed induction generators (DFIGs) have begun to be used more widely [24]. PMSG wind turbines have more highly reliable operations, lower maintenance expenses, and smaller weights with simpler structures than DFIG wind turbines do. Accordingly, this paper focuses on PMSG wind turbines. Maximum power point tracking control is usually employed to maximize the turbine energy-conversion efficiency through the regulation of the rotational speeds of variable-speed wind turbines. Depending on the wind's aerodynamic conditions, the power captured by the wind turbine can be maximized versus rotational speed characteristics by adjusting the coefficient G_p, which represents the aerodynamic

efficiency of the wind turbine and is a function of the tip speed ratio (TSR). The maximum mechanical output power of the wind turbine is then defined as

$$P_{max} = \frac{1}{2}\rho\pi R^2 S_w^3 G_{p,opt}(\beta, \gamma_{w,opt}) \tag{7}$$

The optimal TSR of the mechanical output is given as

$$\gamma_{w,opt} = \frac{\omega_{m,opt} R}{S_w} \tag{8}$$

For the PMSG wind turbine modeled in this paper [24], the maximum value of the power coefficient ($G_{p,opt}$ = 0.4412) is obtained according to the optimal value of the TSR ($\gamma_{w,opt}$ = 6.9) calculated using (8). Because wind farms consist of several PMSG wind turbines, the power coefficient of a wind farm located at bus i is the sum of the active powers generated by the wind turbines, given by

$$P_{WF,i} = \sum_{n=1}^{NT_n} P_{WT,n} \tag{9}$$

3. Proposed Congestion Management Approach

3.1. P-VSCOPF

Power systems, including wind farms, are open systems. This means that any external parameter can influence their functionalities, which can lead to rather uncertain systems. The proposed OPF for CM is implemented as a P-VSCOPF, which is a nonlinear, multi-objective optimization problem. A probabilistic method has been developed using MCSs that apply random sampling of the uncertain parameter probability density function to solve the problems. In our study, a multi-objective OPF is formulated as

$$Min \quad -(w_1)(C_D P_D - C_S P_S) - w_2 \lambda_c \tag{10}$$

The objective function contains both social welfare and maximum loading margins with weighting factors of $w_1 > 0$ and $w_2 > 0$. Here, we assume that $w_1 = (1 - w)$ and $w_2 = w$, (for $0 < w < 1$). The value of the weighting factor is increased so that stability takes precedence over cost. Hence, the system becomes more stable and has higher operating costs.

The equality and inequality constraints for the problem are as follows:

Power flow equations:

$$f(\delta, V, Q_G, P_S, P_D) = 0 \tag{11}$$

$$f(\delta_c, V_c, Q_{G_c}, \lambda_c, P_S, P_D) = 0 \tag{12}$$

Supply and demand bid blocks:

$$P_{S_{\min}} \leq P_S \leq P_{S_{\max}} \tag{13}$$

$$P_{D_{\min}} \leq P_D \leq P_{D_{\max}} \tag{14}$$

Generation reactive power limit:

$$Q_{G_{min}} \leq Q_G \leq Q_{G_{max}} \tag{15}$$

$$Q_{G_{min}} \leq Q_{G_c} \leq Q_{G_{max}} \tag{16}$$

Thermal limit:

$$I_{ij}(\delta, V) \leq I_{ij_{max}} \tag{17}$$

$$I_{ji}(\delta, V) \leq I_{ji_{max}} \tag{18}$$

$$I_{ij}(\delta_c, V_c) \leq I_{ij_{max}} \tag{19}$$

$$I_{ji}(\delta_c, V_c) \leq I_{ji_{max}} \tag{20}$$

Voltage security limit:

$$V_{min} \leq V \leq V_{max} \tag{21}$$

$$V_{min} \leq V_c \leq V_{max} \tag{22}$$

Loading margin:

$$\lambda_{c_{min}} \leq \lambda_c \leq \lambda_{c_{max}} \tag{23}$$

Here, the subscript c represents the system's maximum loading condition. Equation (12) is related to a loading parameter, which guarantees that the system network has the required margin of voltage stability. The generation and load in the present state, with the loading parameter λ_c, are expressed as

$$P_G = P_{G_0} + P_S \tag{24}$$

$$P_L = P_{L_0} + P_D \tag{25}$$

$$P_{G_c} = (1 + \lambda_c + k_{G_c})P_G \tag{26}$$

$$P_{L_c} = (1 + \lambda_c)P_L \tag{27}$$

In the proposed P-VSCOPF-based approach, the critical loadability λ_c can be expressed as a measure of system congestion. The loadability is maximized to receive the impact of the voltage stability limit. Therefore, the total maximum loadability (TML) and the available loading capability (ALC) can be defined, respectively, as

$$TML = (1 + \lambda_c)\sum P_{L_i} \tag{28}$$

$$ALC = \lambda_c \sum P_{L_i} = \lambda_c TTL \tag{29}$$

Here, TTL is the total transaction level at the current operating point. In Equation (29), the ALC is computed for the product of λ_c and TTL.

3.2. Stability Margin

To make the system more robust against voltage-related disturbances, a suitable level of voltage stability should always be maintained in the power system. The continuation method is used as a tool for voltage security studies in [25]. In this work, the VSM is applied to measure the voltage stability, and the load is assumed to be of the constant-power type. Figure 2 illustrates the bifurcation curve between the power and the voltage. In the P-V curve, the maximum value of the loading parameter, from the base case up to the saddle node bifurcation (SNB) point, which is regarded as the voltage collapse point, indicates the VSM, which is described as the loading distance between the base case and the SNB point in voltage collapse:

$$VSM = P_{SNB} - P_{base} \tag{30}$$

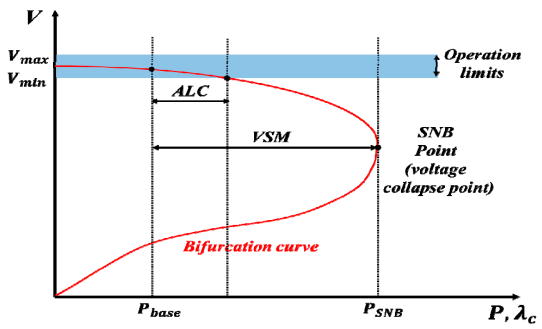

Figure 2. Bifurcation curve for voltage stability analysis.

Equation (30) illustrates that a greater VSM results in a more stable system from a voltage stability viewpoint. On the other hand, a stressed power system typically experiences a low VSM.

3.3. Sensitivity Analysis

3.3.1. VSI Analysis

Steady-state voltage stability analysis includes the determination of an index called the VSI, which is an approximate measure indicating both the most critical bus and the closeness of the system to voltage collapse. To determine the most critical and congested line between buses i and j, contingency ranking is implemented by determining the voltage collapse point from the post-contingency operating conditions. The maximum loading point will move in accordance with variations in both the system topology and the control variables if transmission line outages occur. Since some sensitivity exists between the loading margin and the transmission parameters, a new sensitivity-based branch outage contingency ranking method [26] is used in our study to carry out the contingency selection. This is computed using both the power flow variables and the loading parameter with respect to changes in the transmission line flows. The VSI can be found from the following equation:

$$VSI = \frac{\left|\Delta P_{ij}\right| \bullet \left|P_{ij}\right|}{\left|\Delta \lambda_c\right|} \tag{31}$$

In order to evaluate the weight of each line, a scaling method involving lines with heavy loads is applied. From Equation (31), the contingency line must be the most vulnerable line according to the smallest voltage stability margin. This line is ranked at the top of the list. This technique ranks the contingencies correctly with respect to their impacts on the VSM. The VSI can be used as a real-time operational tool because of its low computational effort requirements. In addition, the VSI is similarly associated with a security cost, which is defined as the amount expended on security improvements to satisfy the $N-1$ criterion. The security cost contains the additional costs incurred by the system to ensure $N-1$ security.

3.3.2. CDF

The optimal location of a wind farm can also be obtained through a sensitivity analysis with respect to the power flow injection of any bus n. This analysis introduces information about the variations in power transfer, and therefore, about loading the system with respect to the variations in the power injection of any bus. This study utilizes these sensitivity factors, called CDFs, which are based on the VSI. The derivation of the CDF is given in Appendix A, and the factors are obtained as

$$CDF_n^{i_c j_c} = \frac{\Delta P_{i_c j_c}}{\Delta P_n} \tag{32}$$

3.4. MOPSO Algorithm

The optimization model of P-VSCOPF involves highly complicated implementations of both the objective and constraint equation differentials. To overcome the major restrictions faced by many traditional methods, evolutionary computation algorithms (e.g., PSO or differential evolution) can be used as reliable alternatives in many complex engineering optimization applications [17]. In this paper, the MOPSO based on the Newton–Raphson method is used as the optimization algorithm for the P-VSCOPF problem. The proposed MOPSO is suitable for solving constrained, nonlinear optimization problems. This technique can be managed easily, and it provides good convergence characteristics with high computing efficiencies compared to conventional PSO. Moreover, it obtains good starting values for the initial population before the PSO process begins by using the Newton–Raphson method. Thus, it offers a better performance in finding the optimal Pareto front.

The velocity and position vectors of a particle in an n-dimensional space are given by

$$X_a = (x_{a1}, \cdots, x_{an}) \tag{33}$$

$$Z_a = (z_{a1}, \cdots, z_{an}) \tag{34}$$

The best position calculated by a particle is

$$Pbest_a = ({x_{a1}}^{best}, \cdots, {x_{an}}^{best}) \tag{35}$$

The particle among all of the particles in the population that has the best position can be represented as

$$Gbest_g = ({x_{g1}}^{best}, \cdots, {x_{gn}}^{best}) \tag{36}$$

The position and velocity of each particle, updated after $(k + 1)$, steps is calculated by

$${X_a}^{(k+1)} = X_a^k + Z_a^{k+1} \tag{37}$$

The velocity of the ith individual during the $(k + 1)$th iteration can be computed by

$$z_{an}^{t+1} = W z_{an}^t + c_1 r_1 (Pbest_{an}^t - x_{an}^t) + c_2 r_2 (Gbest_{gn}^t - x_{an}^t) \tag{38}$$

Finally, the inertia weight parameter W can be expressed as

$$W = (W_i - W_f) \times \frac{(iter_{max} - iter)}{iter_{max}} + W_f \tag{39}$$

Figure 3 shows the MOPSO process. This application is used to check the feasibility of the non-dominated solutions.

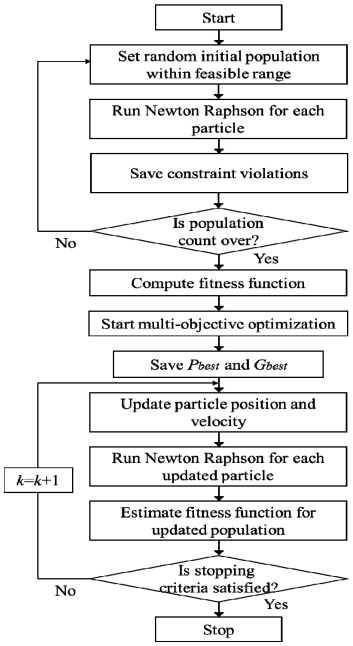

Figure 3. MOPSO procedure.

3.5. Price Analysis

The LMPs are the key factors in both managing the transmission congestion and identifying the spot price. The LMPs are utilized by using a linear programming (LP) approach to compute the power

dispatch schedules while simultaneously maximizing the social welfare function. Network congestion causes LMP differences at the buses. These should be minimized to relieve the congestion while also keeping their values as low as possible. LMPs are commonly associated with both the bidding costs and the dual variables (Lagrange multipliers) of the power flow equation [25]. The Lagrange multiplier is the shadow price for the load flow constraints of the OPF, and it describes each congested transmission line on the network. A higher multiplier means, in general, a greater influence of the corresponding congested transmission line on the prices at each location. Using Equations (10)–(27), the expressions for the LMPs are computed to be

$$\begin{aligned} LMP_{S_i} &= \phi_{P_{S_i}} = C_{S_i} + \mu_{P_{S_{\max_i}}} - \mu_{P_{S_{\min_i}}} - \phi_{cP_{S_i}}(1 + \lambda_c^* + k_{G_c}^*) \\ LMP_{D_i} &= \phi_{P_{D_i}} = C_{D_i} - \phi_{Q_{D_i}} \tan(\varphi_{D_i}) - \mu_{P_{D_{\max_i}}} + \mu_{P_{D_{\min_i}}} \\ &\quad -\phi_{cP_{D_i}}(1 + \lambda_c^*) - \phi_{cQ_{D_i}}(1 + \lambda_c^*) \tan(\varphi_{D_i}) \end{aligned} \tag{40}$$

Equation (40) contains terms related to the loading parameters, which consider the generation marginal cost of the electricity responsible for both supply and demand, including the system losses of each transmission line. Note that the LMPs have additional terms that rely on the voltage security constraints. Thus, these equations represent the manner in which the voltage stability coordinates the existing prices.

This paper also proposes NCPs to both maintain network security parameter limits and send an appropriate signal based on the price of electricity. Equation (40) can be used to perform a decomposition calculation in order to obtain NCPs that are associated with the transmission line limits. The equation to determine the NCP is given as

$$NCP = \left(\frac{\partial f^T}{\partial X}\right)^{-1} \frac{\partial Z^T}{\partial X}(\mu_{max} - \mu_{min}) \tag{41}$$

which shows that the NCPs not only involve transmission congestion but also estimate the degree of congestion severity. After clearing the electricity market from the P-VSCOPF solution, our work uses an LMP payment mechanism for the CM as a cost settlement process that is performed according to the market participants' contributions to both the system congestion and the system losses [26]. In doing so, the total ISO payment is computed as the difference between the supplier and consumer payments as

$$Pay_{ISO} = \sum_i C_{S_i} P_{S_i} - \sum_j C_{D_j} P_{D_j} \tag{42}$$

Overall, the proposed approach is implemented sequentially, as shown in Figure 4.

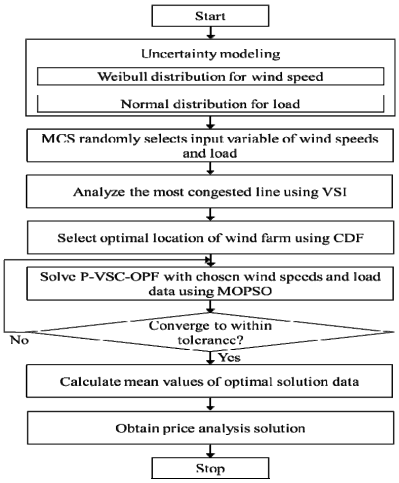

Figure 4. Procedure for proposed approach.

4. Simulation Results

The validity applying of the proposed approach to CM was evaluated using the modified IEEE-24 bus system, as shown in Figure 5. This system consisted of ten generating plants connected by 11 buses, 38 transmission lines, and 17 loads [27], with bus 13 designated as a slack bus. To solve the P-VSCOPF problem, the maximum number of MOPSO algorithm iterations was set to 100. r_1 and r_2 were uniform random factors that were assigned values between 0 and 1 both at each step and for each particle in the swarm in order to add randomness to the velocity update. The inertia weight W was decreased from 0.9 to 0.4 for different iterations. Each of the acceleration coefficients c_1 and c_2 were set equal to 2 in order to achieve a stochastic factor with a mean value of unity. The simulation results were analyzed using the power system analysis toolbox (PSAT) for both MATLAB (version, Manufacturer, City, US State abbrev. if applicable, Country) and GAMS (version, Manufacturer, City, US State abbrev. if applicable, Country) in the optimization package [28].

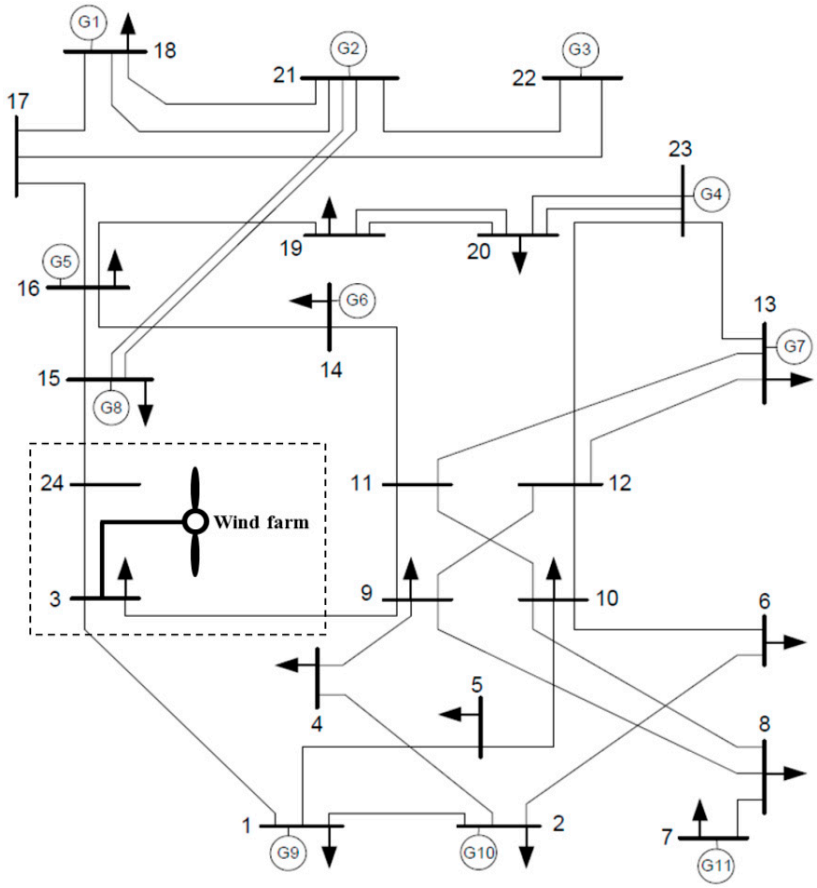

Figure 5. Modified IEEE-24 bus system with a wind farm.

4.1. Probability Distributions of Wind Power and Load

In consideration of the probabilistic variability of both wind speeds and loads, an MCS is conducted to select both the wind power and the system load as input variables. To estimate the Weibull parameters of wind speeds, two years of historical wind speed data were collected from a wind turbine in Seongsan-eup on Jeju Island, South Korea [29]. These data were used as the input for a 2-MW PMSG wind turbine. Our study assumed that wind power generation consumes no fuel. Figure 6 illustrates the cumulative distribution curve of the power output based on a 2-MW wind turbine using an MCS with 1000 samples. The mean value of the wind power output is approximately 1 MW. The normally distributed system load uncertainty is shown in Figure 7. It is considered using

the mean value of the period in which congestion occurs more frequently. For statistical purposes, the normal distribution representing the load uncertainty can be obtained with a standard deviation of 5%.

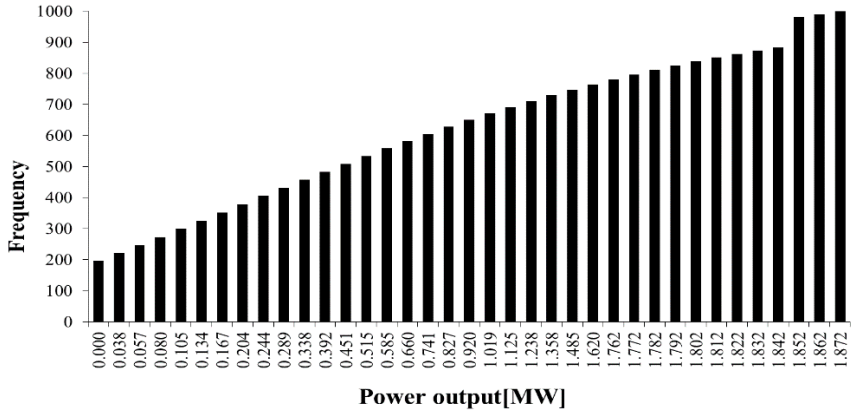

Figure 6. Cumulative distribution curve of wind power.

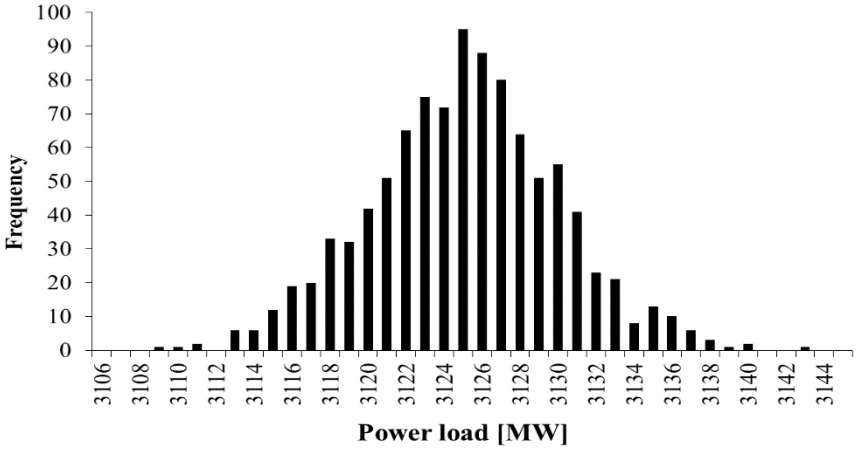

Figure 7. Normally distributed load uncertainty.

4.2. Optimal Locations of Wind Farms

The optimal sites of wind farms with respect to CM were obtained via a CDF based on VSI. In consideration of the contingency analysis, the ten highest transmission-line VSI values were calculated, and the results are shown in Table 1. Note that the line outage between buses 3 and 24 was the most severe because it had the smallest security margin. The critical line, which had the highest security margin value, was considered a potential candidate for CM. These CDFs are obtained based on the VSI data and are given in Table 2. Higher CDFs values indicate that the lines are more critical to power transfer in the transmission lines. Table 2 illustrates that the power injections of bus 3 are the biggest influence on the power flowing through this line. Based on the CDFs results, we find that suitable wind farm locations are typically among the load-side buses. As shown in Figure 5, a wind farm was placed at bus 3, which was the optimal location regarding CM. This wind farm was composed of 300 PMSG wind turbines rated at 2 MW each. The total wind power capacity of 600 MW represented approximately 20% of the total generation capacity.

Table 1. Ranking results and corresponding VSI values.

Rank	Between Buses	VSI
1	3–24	1121.57
2	23–20	735.85
3	17–16	698.50
4	16–14	473.11
5	19–20	475.72
6	19–16	350.73
7	18–17	335.22
8	21–15	304.80
9	10–6	274.51
10	1–2	223.31

Table 2. CDFs for lines between buses 3 and 24.

Bus	CDF	Bus	CDF
1	0.4330	13	−0.0768
2	0.4853	14	−0.3205
3	1.3113	15	−0.7625
4	0.3358	16	−0.634
5	0.0359	17	−0.5492
6	−0.4014	18	−0.5419
7	−0.0498	19	−0.5507
8	0.1511	20	−0.4097
9	0.3992	21	−0.6040
10	0.1580	22	−0.5824
11	−0.0463	23	−0.3308
12	0.0232	24	−1.8239

4.3. Solution Results and Comparison

To verify the effectiveness of the proposed approach, the performances of conventional OPF, VSCOPF, and P-VSCOPF with respect to CM were compared for the modified IEEE-24 bus system. In our study, all three methods were utilized to consider the optimal installation of the wind farm in bus 3, which is obtained through a CDF based on VSI. However, both conventional OPF and VSCOPF, which take into account only the mean values of loads and the wind farm's output, do not consider the probabilistic effects between the loads and the wind farm's variability. Meanwhile, P-VSCOPF consists of two parts: an MCS for selecting both the wind output and load input variables and MOPSO for solving the multi-objective optimization problem. It was implemented based on 1000 MCS trials. Table 3 presents the optimal solution results for P-VSCOPF. Note that these results represent the mean values of 1000 MCS trials based on MOPSO. The power generation (P_G) in bus 3, which was connected to the wind farm, was 295.1 MW. This value was determined by the performance of 1000 MCSs with probabilistic variables taken into account. Figure 8 reveals the estimates of the Pareto optimal front, which relates Pay_{ISO} and the loading parameter λ_c. Note that the Pareto optimal front of the test system exhibits highly nonlinear relationships between the social welfare and the voltage stability margin. A suitable range for the weighting factors is approximated to be 0.4–0.8. In fact, for values smaller than 0.4, system security can almost be ignored, and for values higher than 0.8, market power will happen. On the other hand, with respect to the weighting factors within this range, an importance of between 0.4 and 0.8 was assigned to the voltage security. Therefore, we assume that the results of our work apply to test systems with w = 0.6.

Table 3. Optimal solution results for P-VSCOPF.

Bus	LMP ($/MWh)	NCP ($/MWh)	P_G (MW)	P_D (MW)	Pay_{ISO} ($/h)
1	19.4849	0.1934	172	95.04	−1499.55
2	19.5338	0.2067	172	128.04	−858.71
3	18.7920	0.0381	295.1	158.40	2976.65
4	20.1954	0.3120	0	91.48	1847.48
5	19.9423	0.2783	0	62.48	1245.99
6	20.2911	0.3769	0	119.68	2428.43
7	20.2384	0.3134	220.9	161.22	−1208.19
8	20.6143	0.3823	0	150.48	3102.04
9	19.7676	0.2084	0	154.00	3044.22
10	19.8959	0.2633	0	171.60	3414.13
11	19.7557	0.0982	0	0	0
12	19.7065	0.0519	0	0	0
13	19.5299	0.0000	237.8	233.20	−99.62
14	19.5805	0.0460	0	256.08	5014.17
15	18.7755	−0.2834	167	461.64	5532.00
16	18.9073	−0.2417	155	132.00	−434.87
17	18.5877	−0.3417	0	0	0
18	18.7890	−0.3691	400	439.56	−2176.06
19	19.0499	−0.1925	0	238.92	731.42
20	18.9498	−0.2156	0	168.96	4551.40
21	18.3782	−0.3990	400	0	−3201.76
22	17.9248	−0.5160	300	0	−7351.28
23	18.8138	−0.2532	350	0	−12417.08
24	18.5280	−0.3474	0	0	−7040.64

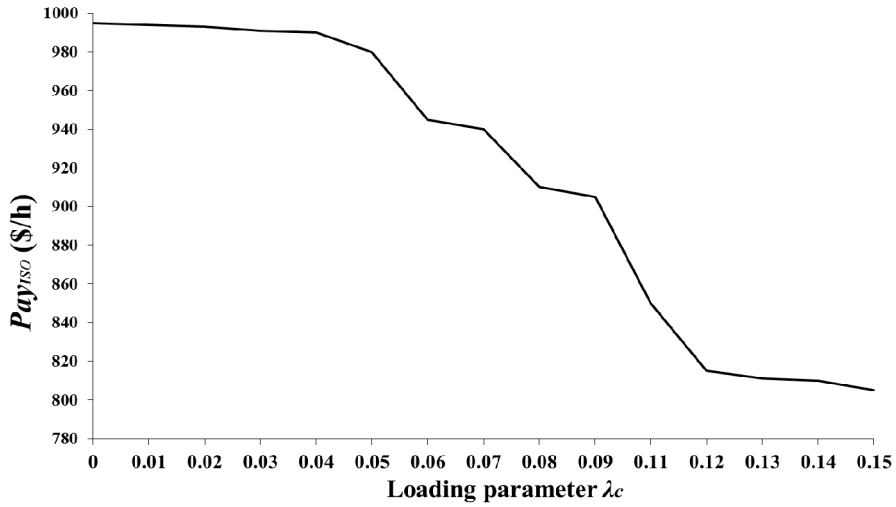

Figure 8. Pareto optimal front for P-VSCOPF.

Figure 9 compares the LMPs and the NCPs. As shown in Figure 9a, for CM, the LMP differences were less with P-VSCOPF than they were with either the conventional OPF or VSCOPF. It is clear that the congestion problems were resolved by minimizing the LMP differences and then maintaining them at the lowest possible levels. As shown in Figure 9b, the range of NCP values was −0.6954 to 0.5962 $/MWh. Here, NCP values at bus 13 (the slack bus) were zero. Lower NCP values indicate lower congestion in the test system. The congestion mitigation of P-VSCOPF was the most effective among those of all of the methods, since the NCP of P-VSCOPF was the lowest. A comparison of the results obtained in each case reveals that the best solution for CM was obtained with P-VSCOPF. Consequently, appropriate realizations of both the voltage stability constraints and the contingency analyses not only result in a better distribution of electricity prices but also reduce the influence of system congestion.

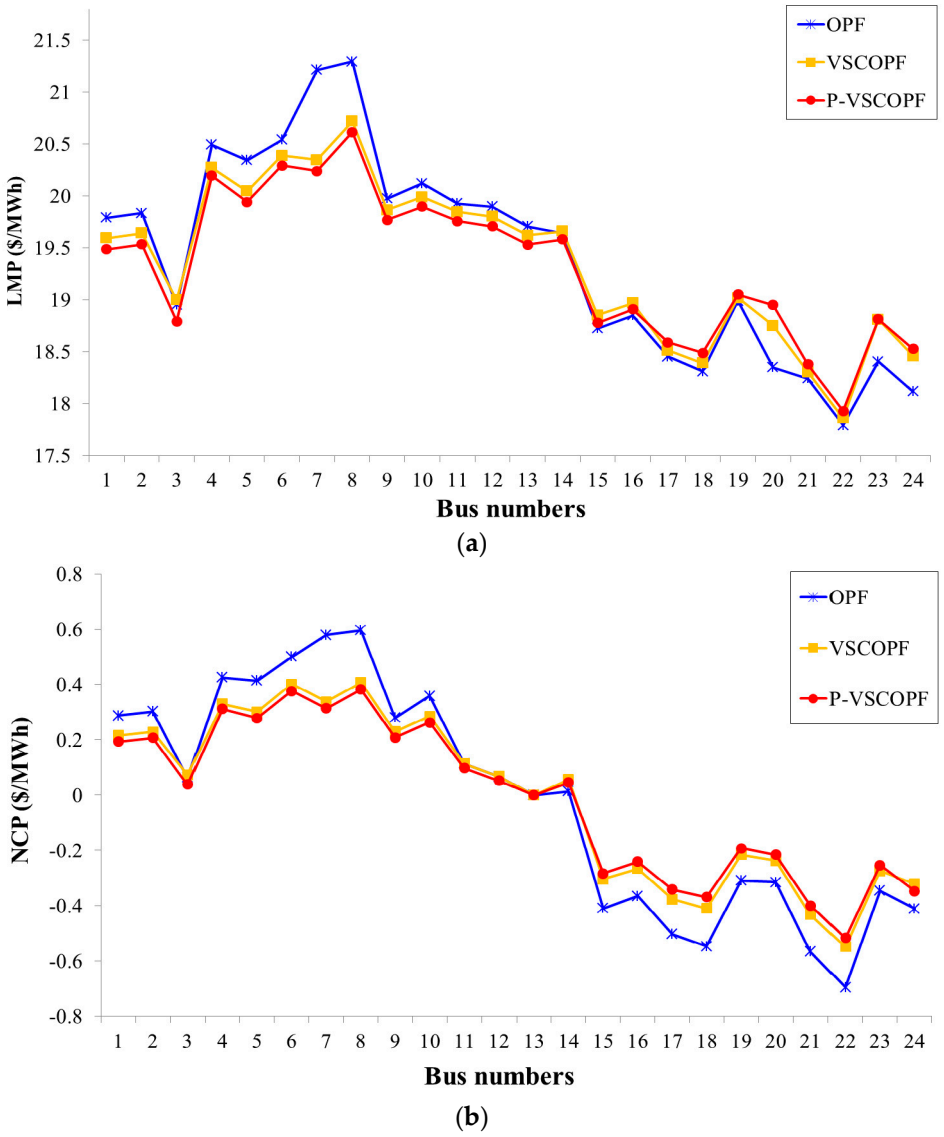

Figure 9. Comparison of optimal pricing for CM. (**a**) LMPs; (**b**) NCPs.

Table 4 shows a comparison of the optimal solutions for the three methods. Compared to both the conventional OPF and the VSCOPF, the proposed approach provides higher values for time to live (TTL), TML, and ALC. The use of enhanced LMPs also results in an improved total ISO payment, although the accrued system losses are higher according to the TTL. Meanwhile, the conventional OPF provides the lowest VSM of 364.37 MW after CM has been applied. Despite the fact that the OPF relives congestion, it does not ensure secure operations of the power network. The stability margin could be low, leading to a vulnerable network. When compared to the OPF, the VSCOPF alleviates congestion, ensuring the power system's security in terms of voltage stability. Nevertheless, the stability margin of VSCOPF remains low after congestion relief has taken place. This means that the total ISO payment should increase because of the additional set of system constraints. In addition, neither the conventional OPF nor the VSCOPF considers the probabilistic effects between the congestion and the wind farm's variability, taking only the mean value of the wind farm's output into account. On the other hand, the proposed approach not only provides the system with a larger VSM of 685.43 MW but can also relieve congestion by considering the margin of the system's stability with respect to the uncertainty in the wind farm. The ISO makes selective payments to both participants that can mitigate congestion as well as those that affect the system stability margin significantly.

To evaluate the ongoing security after CM has been executed, the voltage profiles of the buses for the three methods are shown in Figure 10. The horizontal and vertical axes represent the bus numbers and the voltage magnitudes, respectively. A good voltage profile is one of the indications of a more secure power system. The voltages of P-VSCOPF are the highest among all methods for all of the buses. Thus, P-VSCOPF not only provides a greater stability margin but also leads to a better voltage profile than the other OPF methods do. This means that the system is more robust and can maintain stability even under the most severe circumstances.

Table 4. Comparison of optimal solutions of three methods.

Method	TTL (MW)	System Losses (MW)	TML (MW)	ALC (MW)	Pay_{ISO} ($/h)	VSM (MW)
Conventional OPF	3056.97	52.63	3246.19	189.22	1049.95	364.37
VSCOPF	3139.86	42.39	3555.11	385.25	820.13	640.87
P-VSCOPF	3222.77	41.92	3638.04	415.36	812.26	685.43

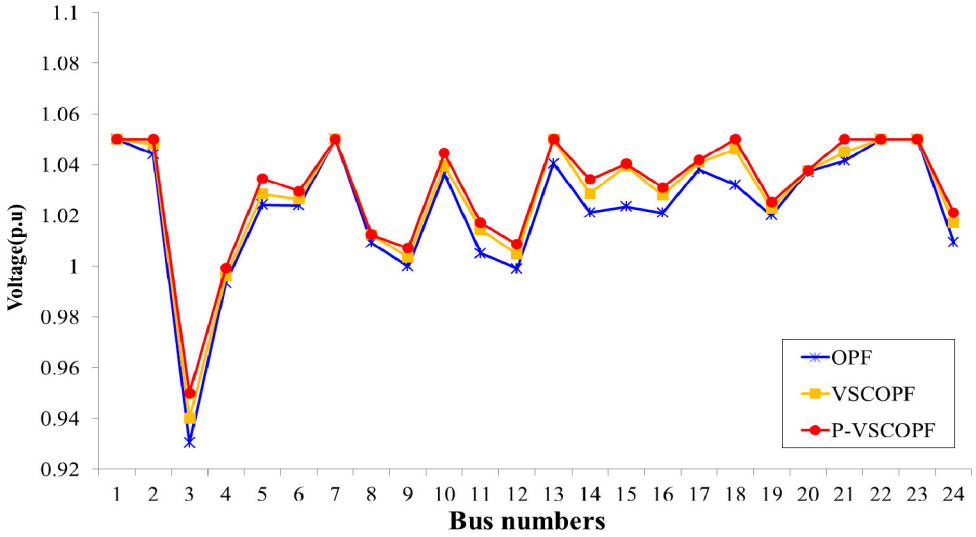

Figure 10. Voltage profiles of three methods.

5. Conclusions

In this paper, a probabilistic, multi-objective approach for CM that considers both voltage stability and wind energy was proposed. P-VSCOPF was formulated as a multi-objective problem not only for maximizing social welfare but also for improving the voltage stability margin. It can be used to assist both ISOs and planners in visualizing the nonlinear relationships between power transfer levels and voltage stability margins via the MOPSO algorithm. MCSs were applied to select the input variables of both wind speed and load by using the probability distribution functions. The problem was solved using 1000 trials of an MCS. The VSI was calculated to increase the accuracy of the sorting and ranking technique in the contingency analysis. The optimal location of a wind farm, with a special emphasis on CM, was also determined using the CDF. The influence of the wind output variations on the congestion price, which is related to both the LMPs and the NCPs, was analyzed. The VSM, ALC, and TML were employed as measures of voltage stability. To illustrate its effectiveness, the proposed approach was both demonstrated and compared to the conventional OPF and VSCOPF using the modified IEEE-24 bus system with wind farms. The simulation results revealed that the P-VSCOPF achieved discernible advantages over all of the other OPF methods. It was able to not only minimize the LMP differences and lower the NCP for CM but also increase the VSM. Therefore, the information provided by the proposed approach can be useful in both the planning and operation of various power systems.

Acknowledgments: This research was supported by Korea Electric Power Corporation through Korea Electrical Engineering & Science Research Institute. (grant number: R15XA03-55).

Author Contributions: Jin-Woo Choi proposed the content of this paper and Mun-Kyeom Kim coordinated the proposed manuscript approach.

Conflicts of Interest: The authors declare no conflict of interest.

Nomenclature

Constants	
ρ	Air density (=1.205 kg/m^2)
$\gamma_{w,opt}$	Optimal tip speed ratio
$G_{p,opt}$	Optimal power coefficient of wind turbine
R	Rotator radius
$\omega_{m,opt}$	Optimal rotational speed
S_{cut-in}	Cut-in speed of wind turbine
S_{rated}	Rated speed of wind turbine
$S_{cut-out}$	Cut-out speed of wind turbine
$P_{\max}, P_{\min}$	Maximum and minimum limits of possible power
$\lambda_{c_{\max}}, \lambda_{c_{\min}}$	Maximum and minimum limits of loading margin
$P_{S_{\max}}, P_{S_{\min}}$	Maximum and minimum limits of supply bid
$P_{D_{\max}}, P_{D_{\min}}$	Maximum and minimum limits of demand bid
$Q_{G_{\max}}, Q_{G_{\min}}$	Maximum and minimum limits of reactive power
$I_{ij_{\max}}$	Maximum limit of line currents between nodes i and j
$V_{\max}, V_{\min}$	Maximum and minimum limits of voltage magnitude
$\mu_{\max}, \mu_{\min}$	Maximum and minimum limits of shadow price
T	Scheduling time (e.g., 24 h)
c_1, c_2	Acceleration coefficients
Variables	
β	Blade pitch angle
S_w	Wind speed
b	Scale parameter of Rayleigh distribution
k, a	Shape and scale parameter of Weibull distribution
σ_L	Standard deviation of load
e_L	Expected value of probability variable
w	Weighting factor
$P_{w,rated}$	Rated power of wind turbine
$P_{WF,i}$	Active power output of wind farm at bus i
$P_{WF,n}$	Active power of nth wind turbine
ΔP_n	Variation in active power of nth bus
P_G, P_L	Power outputs of generator and load, respectively
P_{G_o}, P_{L_o}	Current power outputs of generator and, respectively
P_S, P_D	Supply and demand bid volumes (in MW), respectively
C_S, C_D	Bid prices for supply and demand (in \$/MWh)
Q_G	Generator reactive power
$\Delta P_{i_c j_c}$	Variation of power flow in critical condition
P_{ij}, P_{ji}	Power flowing through lines in both directions
V_i, V_j	Voltage magnitude at buses i and j, respectively
I_{ij}, I_{ji}	Line currents in both directions
P_{SNB}	Power output of SNB point for voltage collapse
P_{base}	Power output at base operating point
δ_i, δ_j	Voltage angle at buses i and j, respectively
θ_{ij}, Y_{ij}	Angle and magnitude of ijth element of Y_{bus}, respectively

λ_c	Loading parameter under critical conditions
k_{G_c}	Loss distribution factor
φ	Lagrange multiplier
μ	Dual variable
φ_{D_i}	Constant load demand power factor angle
X_a^k, Z_a^k	Position and velocity of ith particle at iteration k, respectively
W_i, W_f	Initial and final values of inertia weight
Numbers and Sets	
J_r	Reduced Jacobian matrix
NT_n	Number of wind turbines
k	Number of iterations
$iter_{\max}$	Maximum number of allowed iterations
r_1, r_2	Random numbers between 0 and 1

Appendix A. Derivation of CDF

The real power flow on line k connected between bus i and bus j is formulated as [30]:

$$P_{ij} = |V_i||V_j||Y_{ij}|cos(\theta_{ij} - \delta_i + \delta_j) - V_i^2 Y_{ij}\, cos\, \theta_{ij}. \tag{A1}$$

Applying the approximation of a Taylor series expansion and ignoring the effects of the remaining higher-order terms, Equation (A1) gives

$$\Delta P_{ij} = \frac{\partial P_{ij}}{\partial \delta_i}\Delta\delta_i + \frac{\partial P_{ij}}{\partial \delta_j}\Delta\delta_j + \frac{\partial P_{ij}}{\partial V_i}\Delta V_i + \frac{\partial P_{ij}}{\partial \delta_j}. \tag{A2}$$

Equation (A2) can be rewritten as

$$\Delta P_{ij} = a_{ij}\Delta\delta_i + b_{ij}\Delta\delta_j + c_{ij}\Delta V_i + d_{ij}\Delta V_j. \tag{A3}$$

The coefficients in Equation (A3) are formulated from the partial derivatives of the real power injection corresponding to the variables δ and V and given as

$$a_{ij} = V_i V_j Y_{ij}\, sin(\theta_{ij} + \delta_j - \delta_i), \tag{A4}$$

$$b_{ij} = -V_i V_j Y_{ij}\, sin(\theta_{ij} + \delta_j - \delta_i), \tag{A5}$$

$$c_{ij} = V_j Y_{ij}\, cos(\theta_{ij} + \delta_j - \delta_i) - 2V_i Y_{ij}\, cos\, \theta_{ij}, \tag{A6}$$

$$d_{ij} = V_i Y_{ij}\, cos(\theta_{ij} + \delta_j - \delta_i). \tag{A7}$$

The Newton–Raphson Jacobian relationship is considered in determining the CDFs as

$$\begin{bmatrix} \Delta P \\ \Delta Q \end{bmatrix} = [J]\begin{bmatrix} \Delta\delta \\ \Delta V \end{bmatrix} = \begin{bmatrix} J_{11} & J_{12} \\ J_{21} & J_{22} \end{bmatrix}\begin{bmatrix} \Delta\delta \\ \Delta V \end{bmatrix} \tag{A8}$$

Taking the coupling between ΔP–$\Delta\delta$ and ΔQ–$\Delta\delta$ into consideration and assuming that the reactive power flows are constant (i.e., $\Delta Q = 0$), the power injections variations can be expressed by

$$\Delta P = J_{11}\Delta\delta + J_{12}\Delta V, \tag{A9}$$

$$0 = J_{21}\Delta\delta + J_{22}\Delta V. \tag{A10}$$

Equations (A9) and (A10) then become

$$\Delta P = J_{11}\Delta\delta - J_{12}J_{22}^{-1}J_{21}\Delta\delta = J_r\Delta\delta. \tag{A11}$$

From Equation (A11), the value of the voltage angle variation is given by

$$\Delta\delta = [J_r]^{-1}\Delta P. \tag{A12}$$

From Equation (A10), the voltage variation with respect to the variations in power can be written as

$$\Delta V = J_{22}^{-1}J_{21}\Delta\delta = J_{22}^{-1}J_{21}[J_r]^{-1}\Delta P. \tag{A13}$$

Equations (A12) and (A13) are formulated as

$$\Delta\delta_i = \sum_{l=1}^{n} m_{il}\Delta P_l \quad i = 1, 2, ..., n, \quad i \neq s, \tag{A14}$$

$$\Delta V_i = \sum_{l=1}^{n} m_{ilv}\Delta P_l \quad i = 1, 2, ..., n, \quad i \neq s. \tag{A15}$$

Substituting Equations (A14) and (A15) into Equation (8), the variation in real power flow becomes

$$\Delta P_{ij} = a_{ij}\sum_{l=1}^{n} m_{il}\Delta P_l + b_{ij}\sum_{l=1}^{n} m_{jl}\Delta P_l + c_{ij}\sum_{l=1}^{n} m_{jlv}\Delta P_l + d_{ij}\sum_{l=1}^{n} m_{jlv}\Delta P_l. \tag{A16}$$

Equation (A16) can be rewritten as

$$\begin{array}{rl} \Delta P_{ij} = & (a_{ij}m_{i1} + b_{ij}m_{j1} + c_{ij}m_{i1v} + d_{ij}m_{j1v})\Delta P_1 \\ & +...(a_{ij}m_{in} + b_{ij}m_{jn} + c_{ij}m_{inv} + d_{ij}m_{jnv})\Delta P_n \end{array}. \tag{A17}$$

Thus, the CDF corresponding to both the nth bus and the line ij, connecting buses i and j, can be obtained as

$$\Delta P_{ij} = CDF_1^{ij}\Delta P_1 + CDF_2^{ij}\Delta P_2 + ... + CDF_n^{ij}\Delta P_n, \tag{A18}$$

$$CDF_n^{ij} = a_{ij}m_{in} + b_{ij}m_{jn} + c_{ij}m_{inv} + d_{ij}m_{jnv}. \tag{A19}$$

References

1. Kumar, A.; Srivastava, S.C.; Singh, S.N. Congestion management in competitive power market: A bibliographical survey. *Int. J. Electr. Power Energy Syst.* **2005**, *76*, 153–164. [CrossRef]
2. Méndez, R.; Rudnick, H. Congestion management and transmission rights in centralized electric markets. *IEEE Trans. Power Syst.* **2004**, *19*, 889–896. [CrossRef]
3. Pillay, A.; Karthikeyan, S.P.; Kothari, D. Congestion management in power systems—A review. *Int. J. Electr. Power Energy Syst.* **2015**, *70*, 83–90. [CrossRef]
4. Hong, Y.Y.; Wu, C.P. Day-ahead electricity price forecasting using a hybrid principal component analysis network. *Energies* **2012**, *5*, 4711–4723. [CrossRef]
5. Wang, Q.; Zhang, G.; McCally, J.D.; Zheng, T.; Litvinov, E. Risk-Based Locational Marginal Pricing and Congestion Management. *IEEE Trans. Power Syst.* **2014**, *29*, 2518–2528. [CrossRef]
6. Pandey, S.N.; Tapaswi, S.; Srivastava, L. Growing RBFNN-based soft computing approach for congestion management. *Neural Comput. Appl.* **2009**, *18*, 945–955. [CrossRef]
7. Xie, J.; Wang, L.; Bian, Q.; Zhang, X.; Zeng, D.; Wang, K. Optimal Available Transfer Capability Assessment Strategy for Wind Integrated Transmission Systems Considering Uncertainty of Wind Power Probability Distribution. *Energies* **2016**, *9*, 704. [CrossRef]
8. Tan, A.; Lin, X.; Sun, J.; Lyu, R.; Li, Z.; Peng, L.; Khalid, M.S. A Novel DFIG Damping Control for Power System with High Wind Power Penetration. *Energies* **2016**, *9*, 521. [CrossRef]
9. De Quevedo, P.M.; Contreras, J. Optimal Placement of Energy Storage and Wind Power under Uncertainty. *Energies* **2016**, *9*, 528. [CrossRef]
10. Sood, Y.R.; Singh, R. Optimal model of congestion management in deregulated environment of power sector with promotion of renewable energy sources. *Renew. Energy* **2010**, *35*, 1828–1836. [CrossRef]

11. Deb, S.; Gope, S.; Goswami, A.K. Congestion management considering wind energy sources using evolutionary algorithm. *Electr. Power Compon. Syst.* **2015**, *43*, 723–732. [CrossRef]
12. Ahmadi, H.; Lesani, H. Transmission congestion management through LMP difference minimization: A renewable energy placement case study. *Arab. J. Sci. Eng.* **2014**, *39*, 1963–1969. [CrossRef]
13. Morgan, E.C.; Lackner, M.; Vogel, R.M.; Baise, L.G. Probability distributions for offshore wind speeds. *Energy Convers. Manag.* **2011**, *52*, 15–26. [CrossRef]
14. Aguado, J.A.; Quintana, V.H.; Madrigal, M.; Rosehar, W.D. Coordinated spot market for congestion management of inter-regional electricity markets. *IEEE Trans. Power Syst.* **2004**, *19*, 180–187. [CrossRef]
15. Saini, A.; Saxena, A.K. Optimal power flow based congestion management methods for competitive electricity market. *Int. J. Eng. Comput. Electr. Eng.* **2010**, *2*, 73–80. [CrossRef]
16. Talukdarar, B.K.; Sinhaa, A.K.; Mukhopadhyaya, S.; Bose, A. A computationally simple method for cost-efficient generation rescheduling and load shedding for congestion management. *Int. J. Electr. Power Energy Syst.* **2005**, *77*, 379–388. [CrossRef]
17. Su, H.Y.; Hsu, Y.L; Chen, Y.C. PSO-based voltage control strategy for loadability enhancement in smart power grids. *Appl. Sci.* **2016**, *6*, 449. [CrossRef]
18. Esmaili, M.; Shayanfar, H.A.; Amjady, N. Congestion management considering voltage security of power systems. *Energy Convers. Manag.* **2009**, *50*, 2562–2569. [CrossRef]
19. Milano, F.; Cañizares, C.A.; Invernizzi, M. Multiobjective optimization for pricing system security in electricity markets. *IEEE Trans. Power Syst.* **2003**, *18*, 596–604. [CrossRef]
20. Conejo, A.J.; Milano, F.; García-Bertrand, R. Congestion management ensuring voltage stability. *IEEE Trans. Power Syst.* **2006**, *21*, 357–364. [CrossRef]
21. Pandit, M.; Chaudhary, V.; Dubey, H.M.; Panigrahi, B.K. Multi-period wind integrated optimal dispatch using series PSO-DE with time-varying Gaussian membership function based fuzzy selection. *Int. J. Electr. Power Energy Syst.* **2015**, *73*, 259–272. [CrossRef]
22. Manwell, J.F.; McGowan, J.G.; Rogers, A. *Wind Energy Explained: Theory Design and Application*; John Wiley & Sons: Chichester, UK, 2002.
23. Ramirez, P.; Carta, J.A. Influence of the data sampling interval in the estimation of the parameters of the Weibull wind speed probability density distribution: A case study. *Energy Convers. Manag.* **2005**, *46*, 2419–2438. [CrossRef]
24. Choi, J.W.; Heo, S.Y.; Kim, M.K. Hybrid operation strategy of wind energy storage system for power grid frequency regulation. *IET Gener. Trans. Distrib.* **2016**, *10*, 736–749. [CrossRef]
25. Kim, M.K.; Hur, D. An optimal pricing scheme in electricity markets by parallelizing security constrained optimal power flow based market-clearing model. *Int. J. Electr. Power Energy Syst.* **2013**, *48*, 161–171. [CrossRef]
26. Kim, M.K.; Park, J.K.; Nam, Y.W. Market clearing for pricing system security based on voltage stability criteria. *Energy* **2011**, *36*, 1255–1264. [CrossRef]
27. Kim, S.S.; Kim, M.K.; Park, J.K. Consideration of Multiple Uncertainties for Evaluation of Available Transfer Capability using fuzzy continuation power flow. *Int. J. Electr. Power Energy Syst.* **2008**, *30*, 581–593. [CrossRef]
28. Ferris, M.C. *MATLAB and GAMS: Interfacing Optimization and Visualization Software*; Comuter Sciences Department, University of Wisconsin-Madison: Madison, WI, USA, 2005. Available online: http://www.cs.wisc.edu/math-prog/matlab.html (accessed on 7 April 2017).
29. Min, C.G.; Hur, D.; Park, J.K. Economic Evaluation of Offshore Wind Farm in Korea. *J. Electr. Eng. Technol.* **2014**, *63*, 1192–1198. [CrossRef]
30. Kumar, A.; Srivastava, S.C.; Singh, S.N. A zonal congestion management approach using ac transmission congestion distribution factors. *Electr. Power Syst. Res.* **2014**, *72*, 85–93. [CrossRef]